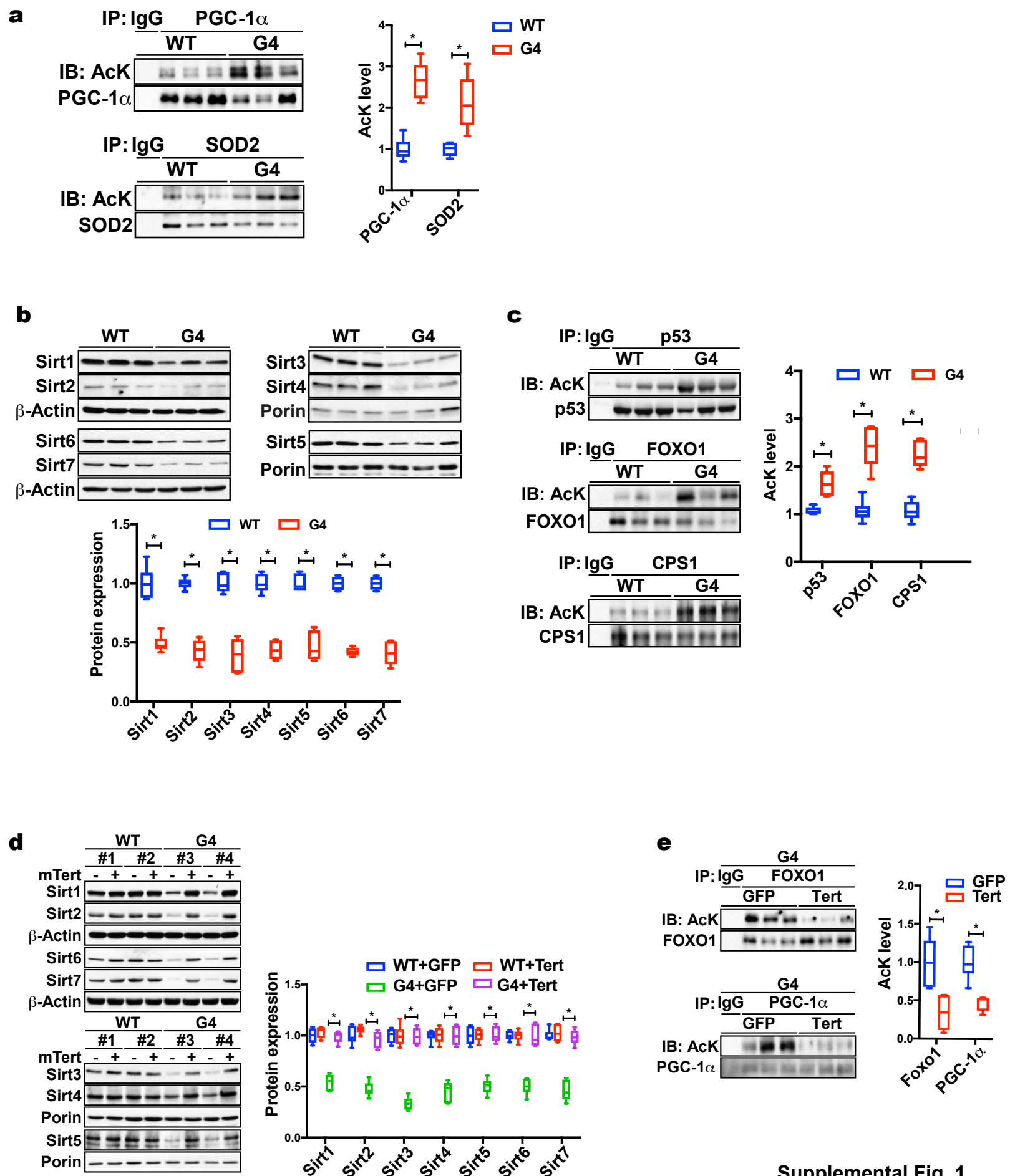


**Supplemental Information**

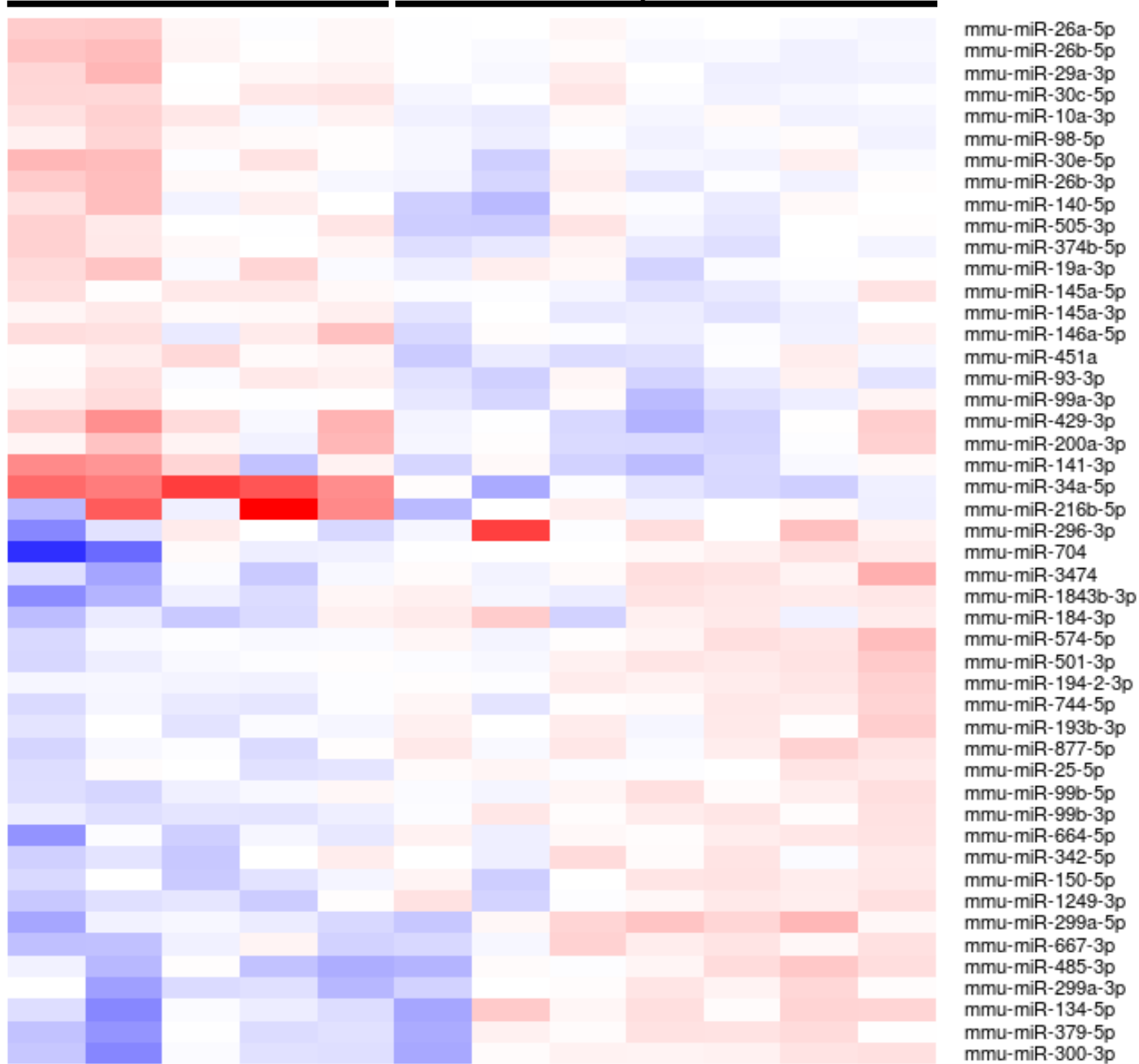
**Telomere Dysfunction Induces Sirtuin**

**Repression that Drives Telomere-Dependent Disease**

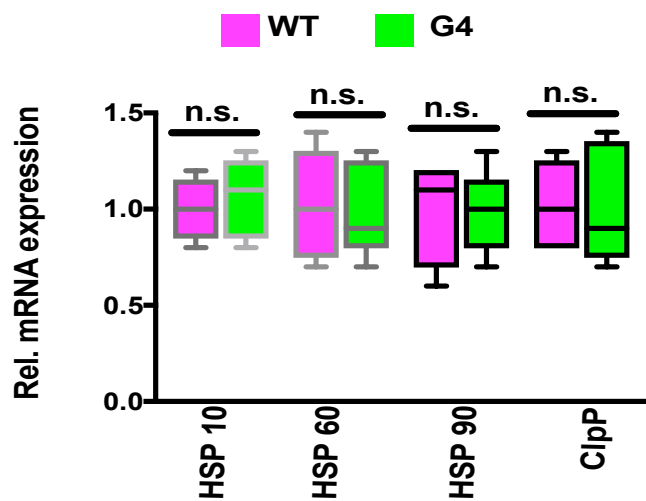
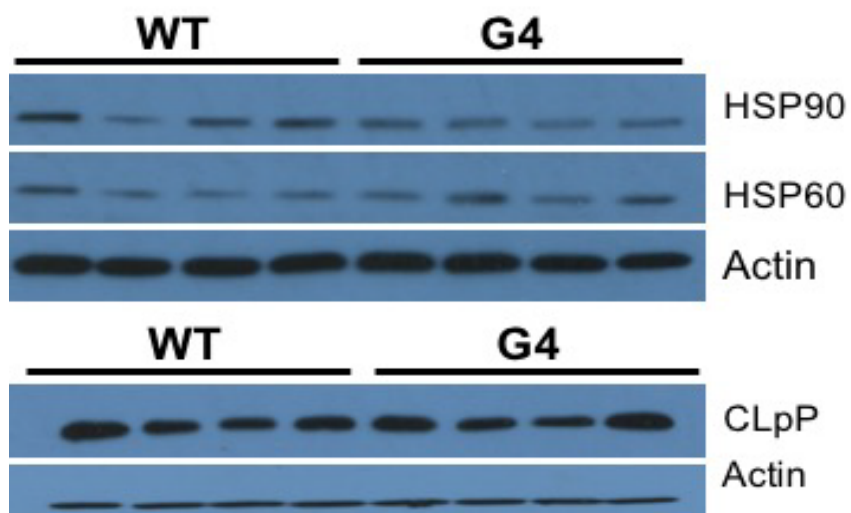
**Hisayuki Amano, Arindam Chaudhury, Cristian Rodriguez-Aguayo, Lan Lu, Viktor Akhanov, Andre Catic, Yury V. Popov, Eric Verdin, Hannah Johnson, Fabio Stossi, David A. Sinclair, Eiko Nakamaru-Ogiso, Gabriel Lopez-Berestein, Jeffrey T. Chang, Joel R. Neilson, Alan Meeker, Milton Finegold, Joseph A. Baur, and Ergun Sahin**



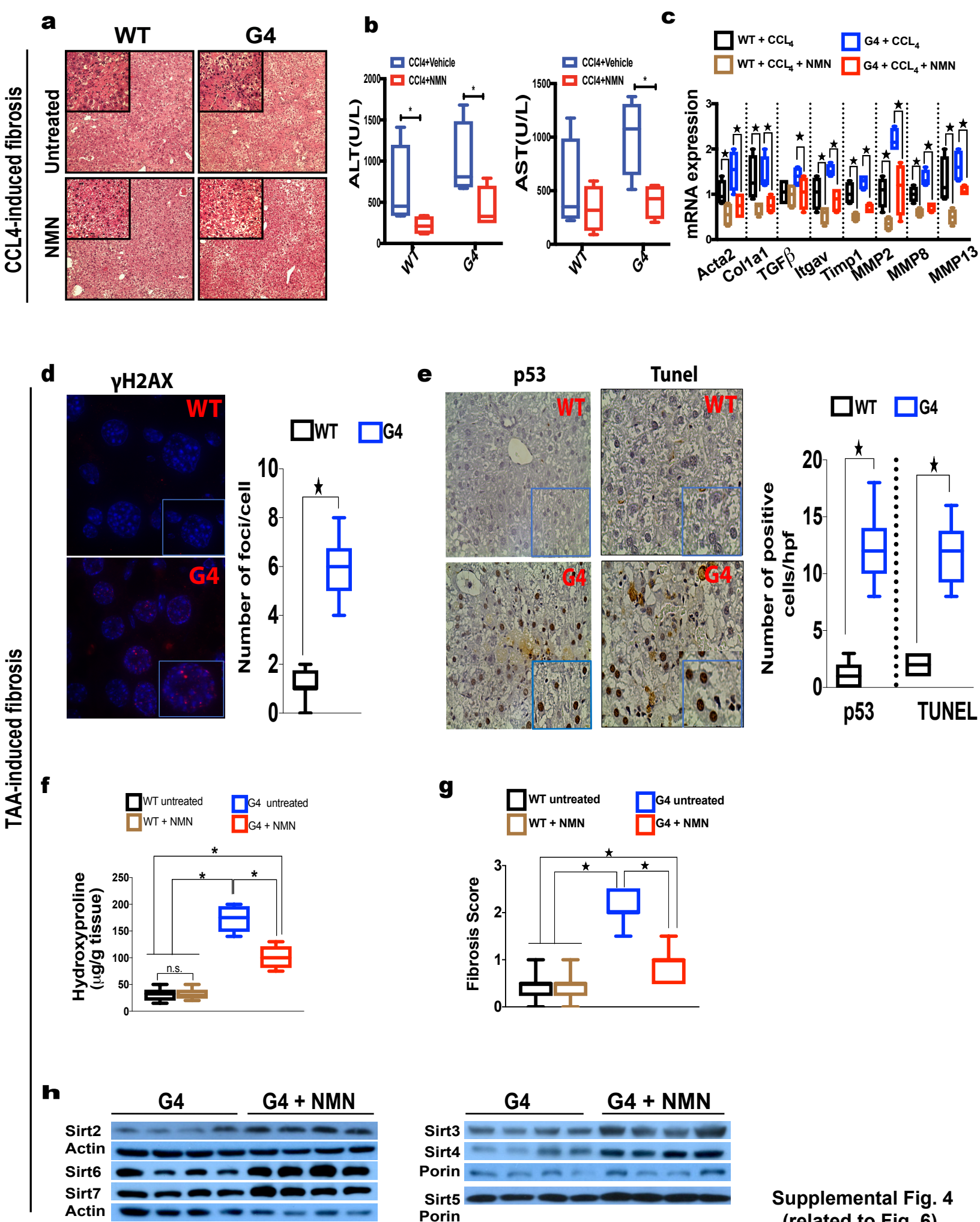
Supplemental Fig. 1  
(related to Fig. 1)

**a****G4****G4/p53 -/-**

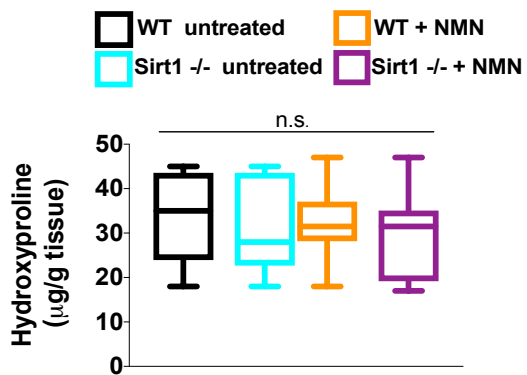
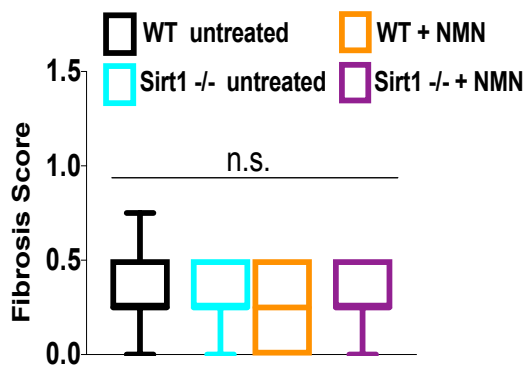
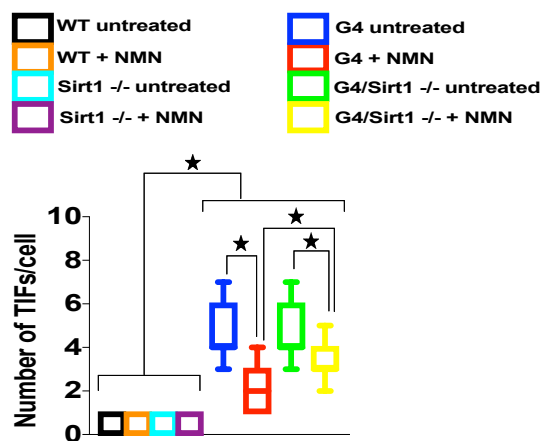
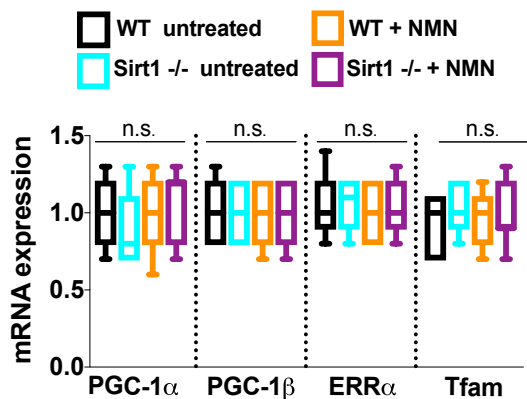
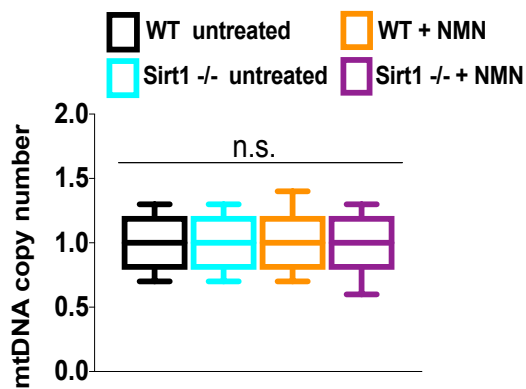
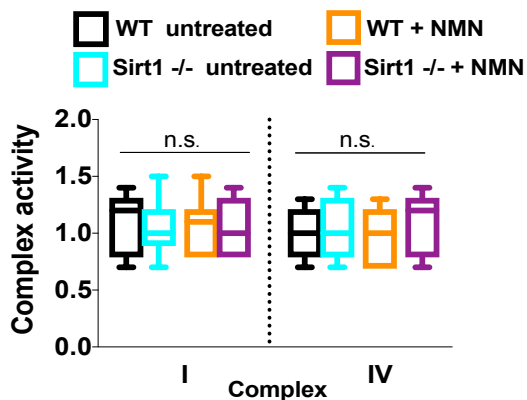
**Supplemental Fig. 2**  
**(related to Fig. 4)**

**a****b**

Supplemental Fig. 3  
(related to Fig. 5)



Supplemental Fig. 4  
(related to Fig. 6)

**a****b****c****d****e****f**

Supplemental Fig. 5  
(related to Fig. 7)

**Supplemental Fig. 1 (related to Fig. 1) Telomere dysfunction induces sirtuin repression in MEFs and liver tissue while telomerase reactivation reverses these changes** (a) IP-western: Pgc-1 $\alpha$  and Sod2 are hyperacetylated in G4 liver compared to WT liver tissue (shown are 3 per group; n= 9 per group; p < 0.05); (b) Western blot analysis demonstrates that sirtuins are repressed in a cell-autonomous manner in G4 MEFs (3 independent cell lines/group; p < 0.05); (c) Combined IP-western blot analysis reveals hyperacetylation of several sirtuin targets (p53, Foxo1, Cps1) in G4 MEFs (3 independent MEF lines/group; p < 0.05); (d) Telomerase reactivation in two WT (#1; #2) and two G4 (#3; #4) MEF cell lines increases sirtuin protein abundance in G4 MEFs without affecting sirtuin levels in WT MEFs; (e) Telomerase reactivation reverses hyperacetylation of PGC-1 $\alpha$  and FOXO1 in three G4 MEF cell lines; Results are quantified by densitometry and expressed as mean  $\pm$  s.e.m.; t-test was used to determine statistical significance with p <0.05 considered as significant, as indicated by (\*).

**Supplemental Fig. 2 (related to Fig. 4) P53 regulates distinct set of miRNAs in G4 mice** (a) Heat map of differentially regulated miRNAs in G4/p53 +/+ (n= 5) and G4/p53 -/- (n= 6) liver tissue as determined by RNA sequencing; (b) RT-qPCR-based analysis of p53-dependent miRNAs in liver tissue of WT and G4 mice (n= 8 per group). Results are expressed as mean  $\pm$  s.e.m.; t-test was used to determine statistical significance with p <0.05 considered as significant, as indicated by (\*).

**Supplemental Fig. 3 (related to Fig. 5) Telomere dysfunction is not associated with activation of mtUPR response in the liver** (a) RT-qPCR analysis of WT or G4 liver tissue does not show changes in expression levels of mtUPR markers heat shock protein HSP 10, 60, 90 and protease ClpP (n= 4 per group; t-test was used to determine statistical significance); (b) Western blot analysis of mtUPR markers does not show any difference between WT and G4 mice (n= 4 per group)

**Supplemental Fig. 4 (related to Fig. 6)** (a) Representative H&E staining of liver section derived from WT and G4 mice shows that NMN treated mice have less necrosis (see insert for blow-up of necrotic areas; n= 12 per group); (b) Liver transaminase (ALT, AST) levels in peripheral blood are decreased in mice treated with NMN indicative of decreased liver cell damage (n= 12 per group); (c) RT-qPCR analysis demonstrates decreased expression of fibrosis-associated genes in mice treated with NMN (n= 12 per group); (d, e)  $\gamma$ H2AX, p53 and TUNEL staining show minimal effect of TAA in WT mice compared to G4 mice; graphs on the right show quantification of  $\gamma$ H2AX foci per cell and number of p53 or TUNEL positive cells per high-power field; (n = 8 per group; for  $\gamma$ H2AX determination a total of 50 cells per mouse were scored from 5 randomly chosen liver sections and for p53 and TUNEL the number of positive cells were determined from 5 random section and counted per high-power field per mouse); (f) Hydroxyproline determination shows minimal collagen accumulation in TAA-treated WT mice compared to G4 mice, which was significantly reduced with NMN treatment (n= 8 mice per group); (g) Quantification of fibrosis shows TAA induces minimal fibrosis in WT mice while G4 mice develop marked fibrosis, which is significantly improved with NMN treatment (n= 8 mice per group); (h) Western blot analysis of G4 mice subjected to TAA shows significant increase of sirtuins in mice treated with NMN (shown are 4 mice of 8 total analyzed). Results are expressed as mean  $\pm$  s.e.m.; t-test was used to determine statistical significance with p <0.05 considered as significant, as indicated by (\*).

**Supplemental Fig. 5 (related to Fig. 7) NMN has no effect in TAA- treated wild type mice with preserved telomeres** (a, b) TAA treatment has little effect on fibrosis development in WT mice after 4 week of treatment as indicated by (a) low hydroxyproline and (b) fibrosis score, which is not altered by NMN treatment; (c) number of telomere-induced foci (TIF's) per cell is reduced with NMN treatment in G4 mice and this is blunted in the absence of Sirt1; WT mice have very few TIFs and this is not impacted by NMN; (d-f) NMN does not affect (d) mitochondrial biogenesis factors, (e) mtDNA copy number and (f) complex I and IV activity (in mice with preserved telomeres, irrespective of Sirt1 status; (n= 8 per group). Results are expressed as mean  $\pm$  s.e.m.; t-test was used to determine statistical significance with p <0.05 considered as significant, as indicated by (\*).